

## Energetics approach to predicting mortality risk from environmental stress: a case study of coral bleaching

**Kenneth R.N. Anthony<sup>1</sup>, Mia O. Hoogenboom<sup>2</sup>, Jeffrey A. Maynard<sup>3</sup>, Andréa G. Grottoli<sup>4</sup> and Rachael Middlebrook<sup>1</sup>**

<sup>1</sup>Centre for Marine Studies, and ARC Centre of Excellence for Coral Reef Studies, The University of Queensland, St Lucia, Qld 4072, Australia; <sup>2</sup>Centre Scientifique de Monaco, Avenue St Martin, MC 98000, Monaco; <sup>3</sup>Applied Environmental Decision Analysis CERF Hub, School of Botany, University of Melbourne, Parkville, VIC 3010, Australia; and <sup>4</sup>Ohio State University, School of Earth Sciences, 125 South Oval Mall, Columbus, OH 43210, USA

### Summary

1. Coral bleaching events, predicted to increase in frequency and severity as a result of climate change, are a threat to tropical coral-reef ecosystems worldwide. Although the onset of spatially extensive, or 'mass', bleaching events can be predicted using simple temperature stress metrics, no models are available for predicting coral mortality risk or sub-lethal stress associated with bleaching. Here, we develop a model that links the functional response of colony energy balance and energy-store dynamics to coral mortality risk and recovery during and following bleaching events.
2. In a series of simulations using response functions and parameter values derived from experimental studies for two Indo-Pacific coral species (*Acropora intermedia* and *Montipora monasteriata*), we demonstrate that prior energy-costly disturbances and alternative energy sources are both important determinants of coral mortality risk during and following bleaching.
3. The timing of the onset of coral mass mortality is determined by a combination of bleaching severity (loss rate of photopigments), duration of the bleaching event, heterotrophy and the size of energy reserves (as lipid stores) before bleaching occurs.
4. Depending on initial energy reserves, model results showed that high rates of heterotrophy could delay the onset of coral mortality by up to three weeks. Survival following bleaching was also strongly influenced by remaining lipid reserves, rates of heterotrophy, and rates of photopigment (or symbiont) recovery.
5. Our results indicate that energy-costly disturbances and low availability of food, before and during bleaching events, respectively, work to increase bleaching-induced coral mortality risk for acroporid corals on Indo-Pacific reefs.

**Key-words:** climate change, environmental stress, physiological energetics, scleractinian coral, great barrier reef

### Introduction

Over the past decade, most coral reefs around the world have been affected by mass bleaching events (Marshall & Shulterberg 2006). Even under the most conservative climate change scenarios, predictions for the coming decades suggest that coral reefs could eventually undergo bleaching annually (Hoegh-Guldberg 1999; Donner *et al.* 2007). Concern about

the ecological and economic implications of broad-scale reef degradation has motivated a growing number of studies into how water temperature (Berkelmans 2002; Berkelmans *et al.* 2004) and interacting factors such as solar radiation (Brown *et al.* 1994), water quality (Anthony *et al.* 2007), and a suite of associated factors (Maina *et al.* 2008) trigger and sustain coral bleaching events. Although a number of studies have demonstrated relationships between bleaching, growth and mortality in corals (Loya *et al.* 2001; McClanahan 2004) no current models can be used to predict the extent of bleaching-induced coral mortality at any spatial scale. This is due to the functional link between the bleaching response and the physiological downstream processes that lead to mortality

\*Correspondence author: E-mail: k.anthony@uq.edu.au

Re-use of this article is permitted in accordance with the Creative Commons Deed, Attribution 2.5, which does not permit commercial exploitation.

not, as of yet, being effectively accounted for. Indeed, the satellite-based applications available that monitor sea surface temperature and the accumulation of heat stress can only predict the onset (Gleason & Strong 1995; Strong *et al.* 2004) and in a few cases the severity (Maina *et al.* 2008; Maynard *et al.* 2008) of bleaching events. Given climate change scenarios it is, however, increasingly important to develop and refine the ability to predict the risk of coral mortality during and following environmental stress events in order to better predict shifts in community composition.

Organism energetics allows insight into how the processes of environmental stress, physiological response and mortality are inter-related (Gurney *et al.* 1996). For all organisms, energy flow provides an important currency for physiological performance, including maintenance, growth and reproduction – all of which have implications for survival and fitness (Maltby 1999). A growing number of studies have used energetics as a framework for linking sub-organism processes to population ecology in unitary organisms (Noonburg *et al.* 1998; Koijman 2000; Nisbet *et al.* 2000, 2004). Only a few studies, however, have applied this framework to clonal photosymbiotic organisms like corals (Anthony *et al.* 2007; Hoogenboom *et al.* 2008).

The energy status of an organism is a function of (i) the current and past energy intakes and losses, and (ii) growth rate and energy allocation between maintenance, growth and reproduction (reviewed by Koijman 2000). In corals, energy acquisition by the holobiont is largely determined by rate of photosynthetic carbon fixation, rate of respiration, carbon transfer by symbionts (Spencer-Davies 1984; Muscatine 1990; Grottoli *et al.* 2006) and heterotrophy by the host (Sebens *et al.* 1996; Ferrier-Pages *et al.* 1998; Anthony & Fabricius 2000; Houlbrèque *et al.* 2004; Grottoli *et al.* 2006; Borell *et al.* 2008). The dynamics of energy availability and reserves, therefore, influence whether a period of resource scarcity increases the risk of mortality. Coral bleaching is a

special case of resource scarcity in that the capacity for energy acquisition is reduced as the concentration of algal symbionts (and/or photopigments), and thereby photosynthetic capacity of the symbiosis, declines. Whether a given bleaching response leads to mortality depends on: (i) the duration of the stress event, (ii) the energy efficiency of the symbiosis (i.e. the contribution of zooxanthellae-acquired carbon to animal respiration (CZAR, *sensu* Muscatine *et al.* 1981), (iii) the availability of heterotrophic resources, and (iv) the heterotrophic feeding capacity of the coral species (i.e., the contribution of heterotrophic carbon to animal respiration (CHAR, *sensu* Grottoli *et al.* 2006). Consequently, highly heterotrophic coral species in plankton-rich environments may be less critically impacted by loss of photo symbionts than predominantly phototrophic species. Also, some coral species become more heterotrophic during bleaching and recovery (Grottoli *et al.* 2006; Rodrigues & Grottoli 2006).

The purpose of this study is to develop a coupled energetics and mortality risk model for coral symbioses based on the functional links between the bleaching response (i.e. loss of photo-symbionts or pigments), productivity, energy stores and risk of bleaching-induced mortality. The resultant energy-budget model works as a predictive framework and provides insight into the influence that heterotrophic feeding and prior energy-costly disturbances have on mortality risk during and following bleaching events.

## Methods

This section has been divided into three components: 1) model development, 2) functional response calibration, and 3) model simulations. To facilitate interpretation and understanding of the modelling the text has been complemented with two summary tables (Tables 1 and 2) and a figure (Fig. 1) and Supporting Information (Appendix S1) providing details of mathematical solutions to

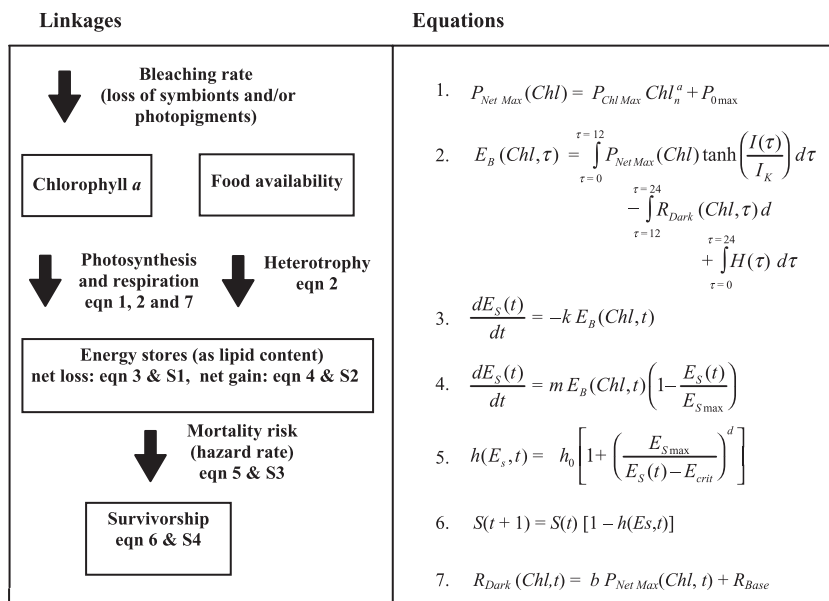


**Fig. 1.** Summary diagram of the coupling of functional response models for coral energetics (photosynthesis, heterotrophy and respiration), energy stores (as lipids) and mortality. Boxes represent state variables and arrows represent processes or rates. Parameter estimates are given in Table 2.

**Table 1.** Variables and parameters used in functional response models

Symbol	Unit	Interpretation
$t$	d	Time in days
$\tau$	h	Time of day in hours
Chl	$\mu\text{g cm}^{-2}$	Chlorophyll <i>a</i> concentration
Chl <sub>Max</sub>	$\mu\text{g cm}^{-2}$	Maximum chlorophyll <i>a</i> concentration
$I(\tau)$	$\mu\text{mol m}^{-2} \text{s}^{-1}$	Solar irradiance as a function of time of day
$I(t)$	$\mu\text{mol m}^{-2} \text{s}^{-1}$	Average daily irradiance
$I_k$	$\mu\text{mol m}^{-2} \text{s}^{-1}$	Sub-saturation irradiance for photosynthesis
$P_{\text{Net Max}}$	$\mu\text{g C cm}^{-2} \text{h}^{-1}$	Maximum hourly rate of net photosynthesis
$P_{\text{Chl Max}}$	$\mu\text{g C cm}^{-2} \text{h}^{-1}$	Rate of net photosynthesis at Chl <sub>Max</sub>
$P_0 \text{Max}$	$\mu\text{g C cm}^{-2} \text{h}^{-1}$	Rate of net photosynthesis (respiration) at Chl = 0
$a$	dimensionless	Exponent relating $P_{\text{Net Max}}$ to Chl
$R_{\text{Dark}}$	$\mu\text{g C cm}^{-2} \text{h}^{-1}$	Rate of respiration in darkness
$R_{\text{Dark Base}}$	$\mu\text{g C cm}^{-2} \text{h}^{-1}$	Baseline rate of dark respiration at zero $P_{\text{Net Max}}$
$B$	dimensionless	Coefficient relating $R_{\text{Dark}}$ to $P_{\text{Net Max}}$
$H(t)$	$\mu\text{g C cm}^{-2} \text{h}^{-1}$	Rate of heterotrophy
$E_B(\text{Chl}, \tau)$	$\mu\text{g C cm}^{-2} \text{h}^{-1}$	Hourly energy budget (as carbon fixation)
$E_B(\text{Chl}, t)$	$\mu\text{g C cm}^{-2} \text{d}^{-1}$	Daily energy budget (as carbon fixation)
$E_S(t)$	$\text{mg cm}^{-2}$	Size of energy stores (as lipid content)
$E_{S \text{Max}}$	$\text{mg cm}^{-2}$	Maximum size of energy stores (carrying capacity)
$E_{S \text{Crit}}$	$\text{mg cm}^{-2}$	Minimal size of energy stores (critical for survival)
$k$	$\text{mg lipid mg C}^{-1}$	Conversion from lipid to respiration rate
$m$	dimensionless	Conversion from photosynthetic rate to lipid content
$h_0$	$\text{d}^{-1}$	Baseline hazard rate, daily percentage decrease in population size
$h(t)$	$\text{d}^{-1}$	Hazard rate function, daily percentage decrease in population size
$d$	dimensionless	Exponent relating hazard rate to lipid content
$\gamma$	dimensionless	Intrinsic rate of chlorophyll increase during recovery

**Table 2** Parameter estimates used in simulations of coral bleaching and mortality-risk responses. See Table 1 for descriptions and units of variables

Parameter	Estimate	Species	Source
Chl <sub>Max</sub>	7 (2) 12 (3)	<i>A. palmata</i> <i>A. intermedia</i>	Fitt <i>et al.</i> 2000 Anthony <i>et al.</i> 2007
$a$	0.30 (0.04) 0.55 (0.09)	<i>M. monasteriata</i> <i>A. formosa</i>	This study
$P_{\text{Chl Max}}$	38.2 (2.3) 70.9 (16.1)	<i>M. monasteriata</i> <i>A. formosa</i>	This study
$b$	0.19 (0.04) 0.18 (0.04)	<i>M. monasteriata</i> <i>A. formosa</i>	This study
$R_{\text{Base}}$	7.22 (0.92) 4.70 (0.67)	<i>M. monasteriata</i> <i>A. formosa</i>	This study
$H(t)$	0.2–3.3 0.2–3.3	<i>A. millepora</i> <i>M. capitata</i>	Anthony, 2000 Grottoli <i>et al.</i> 2006
$E_{S \text{Max}}$	~2.0	<i>A. intermedia</i>	Anthony <i>et al.</i> 2007
$k$	0.455	generic	Spencer-Davies 1991
$m$	0.225	assumed to be $k/2$ for both genera	Gnaiger & Bitterlich 1984
$h_0$	0.00036 (0.00020)	<i>A. intermedia</i>	This study Anthony <i>et al.</i> 2007
$d$	3.01 (0.38)	<i>A. intermedia</i>	This study

some equations. Throughout, we have used data on physiological responses for three coral species from the family Acroporidae, which is one of the dominant groups of reef builders in the Indo-Pacific (Veron 2000). The species used include: *Acropora formosa* and *A. intermedia* (Orpheus Island, Central Great Barrier Reef, GBR) and

*Montipora monasteriata* (Heron Island, southern GBR). All experiments (8-week duration) on bleaching state, oxygen respirometry, lipid stores and mortality responses were carried out in control-environment aquarium facilities at the two island research stations (for details see Anthony *et al.* 2007).

## MODEL DEVELOPMENT

*Functional relationship between energy balance and bleaching*

We describe the bleaching state of corals using concentrations of chlorophyll *a* within coral tissue *Chl*, as a metric for the bleaching response. Rate of bleaching was not modelled here as an explicit function of environmental variables because coral bleaching is a complex function of multiple interacting proximate factors (Maina *et al.* 2008) including temperature (Strong *et al.* 2004), light (Dunne *et al.* 1994), water quality (Anthony *et al.* 2007), season and acclimatization state (Berkelmans & Willis 1999; Weeks *et al.* 2008), as well as zooxanthellae type (Baker 2001; Berkelmans & van Oppen 2006). Instead, bleaching rate was here used as an input (state) variable, assuming a linear decrease in chlorophyll *a* concentrations over time. This is consistent with experimental data for bleaching responses in *A. intermedia* on the Great Barrier Reef (Anthony *et al.* 2007) and in *Porites compressa* and *M. capitata* in Hawaii (Rodrigues *et al.* 2008). We used bleaching rates ranging from 0% to 10% reduction in chlorophyll *a* per day relative to full pigmentation, which is consistent with the reported range of bleaching severities for *Acropora* during major thermal bleaching events on the Great Barrier Reef (Berkelmans *et al.* 2004; Maynard *et al.* 2008).

We then model energy balance as a function of chlorophyll *a* content,  $E_B(Chl, t)$ , as determined by rates of photosynthesis, respiration and heterotrophy and subsequently model the size of energy stores,  $E_S(t)$  as a function of energy balance. Finally, we model mortality risk,  $h(t)$ , as a function of  $E_S(t)$ . The daily energy balance, of corals is governed by rates of photosynthesis, heterotrophy, respiration and excretion (Muscatine 1973, 1990; Anthony & Connolly 2004). Photosynthetic capacity is related to bleaching status via changes in symbiont performance under varying densities and/or varying concentrations of chlorophyll *a* per symbiont in the host (e.g. Porter *et al.* 1989a; Dove *et al.* 2006; Rodrigues & Grottoli 2007). At high symbiont densities (or photopigment concentrations), self-shading is pronounced (Falkowski *et al.* 1990) and small changes in pigment concentrations are likely to have negligible effects on whole-colony rates of photosynthesis (Hoogenboom *et al.* 2008). Conversely, in partially bleached corals, enhanced light scattering by the skeleton may lead to supra-optimal light conditions for the remaining symbionts (Enriques Mendez & Iglesias-Prieto 2005), causing further breakdown of the symbiosis (Hoegh-Guldberg & Jones 1999; Lesser & Farrell 2004). Based on these observations, photosynthetic capacity of unbleached corals can be expected to be insensitive to small reductions in symbiont or photopigment concentrations due to self-shading, but will decrease rapidly when the remaining symbionts (or pigments) are fully light-saturated and in decline. As a measure of photosynthetic capacity, we here use maximum rate of net photosynthesis,  $P_{\text{Net Max}}$ , a key parameter in the photosynthesis-irradiance model (Chalker, Dunlap & Oliver 1983; Barnes & Chalker 1990). In absence of a theory formally relating  $P_{\text{Net Max}}$  to photopigment concentration we use a generic model that qualitatively represents a range of decelerating functional responses

$$P_{\text{Net Max}}(\text{Chl}) = P_{\text{Chl Max}} \text{Chl}_n^a + P_{0 \text{ max}} \quad \text{eqn 1}$$

where  $\text{Chl}_n$  is the concentration of chlorophyll *a* normalized (and non-dimensionalized) to the maximum,  $P_{\text{Chl Max}}$  is the rate of net photosynthesis at the maximum chlorophyll *a* concentration,  $P_{0 \text{ max}}$  is the rate of net photosynthesis for completely bleached corals, and  $a$  is a dimensionless scaling exponent.

*Role of heterotrophy in offsetting energy loss in bleached corals*

Photosynthesis and respiration generally account for the majority of the energy balance in healthy reef-building corals (Muscatine 1990). However in unbleached Hawaiian corals *P. compressa*, *P. lobata* and *Montipora lobata*, heterotrophy accounts for 15–60% of the daily metabolic demand and in *M. capitata* over 100% of the host's energy requirements can be met by heterotrophy during bleaching events (Grottoli *et al.* 2006). Additional research is needed to determine whether such trophic plasticity during bleaching is a universal pattern. Rate of heterotrophic energy acquisition in corals varies strongly among species, health status, food type and environment (Sebens *et al.* 1997; Ferrier-Pages *et al.* 1998; Anthony & Fabricius 2000; Palardy *et al.* 2005; Grottoli *et al.* 2006). Rate of coral heterotrophy ranges from < 1 µg dry wt cm<sup>-2</sup> h<sup>-1</sup> (Anthony 1999; Palardy *et al.* 2008) to more than 20 µg dry wt cm<sup>-2</sup> h<sup>-1</sup> depending on food type, food availability and flow (Sebens *et al.* 1997; Ferrier-Pages *et al.* 1998; Anthony 2000), and temperature (Palardy *et al.* 2005). Assuming a 33% organic carbon content of zooplankton in the size range of prey typically eaten by corals (200–400 µm, Grottoli *et al.*, 2006) and an assimilation efficiency of 50–90% depending on feeding rate (Anthony 2000), this range of ingestion rates corresponds to carbon acquisition rates of between 0.2 and 3.3 µg cm<sup>-2</sup> h<sup>-1</sup>. There is no formal theory describing how changes in photosynthetic capacity may influence rates of heterotrophic feeding  $H(t)$ . Rather than modelling the increase in heterotrophy as a functional response to bleaching (trophic plasticity), we here examine how sensitive bleaching-induced mortality risk is to contrasting rates of heterotrophy based on experimental data and data derived from laboratory and field studies on corals exposed to natural concentrations of zooplankton or other particulate matter (see Table 2).

Rate of excretion in corals can vary between 10% (Anthony & Connolly 2004) and 40% (Crossland *et al.* 1980) of the daily assimilated carbon, depending on environmental conditions (e.g. light, nutrient and sediment regime). However, because rate of excretion correlates with rate of respiration (Anthony & Connolly 2004) we here consider excretion to be part of the respiration response. The daily energy (carbon) budget is here represented by the accumulated daily net rate of photosynthesis during hours of sunlight, accumulated rates of respiration during the night, and accumulated rates of heterotrophy over the 24-h cycle:

$$E_B(\text{Chl}, \tau) = \int_{\tau=0}^{\tau=12} P_{\text{Net Max}}(\text{Chl}) \tan h\left(\frac{I(\tau)}{I_k}\right) d\tau - \int_{\tau=12}^{\tau=24} R_{\text{Dark}}(\text{Chl}, \tau) d\tau + \int_{\tau=12}^{\tau=24} H(\tau) d\tau \quad \text{eqn 2}$$

where  $\tau$  is time in hours after dawn and  $I(\tau)$  is irradiance as a function of time of day using 12-h diurnal light profiles and  $I_k$  is the sub-saturation parameter indicating state of photoacclimation (Anthony & Hoegh-Guldberg 2003a).  $R_{\text{Dark}}(\text{Chl}, \tau)$  is the hourly rate of respiration in darkness (assuming 12 h per day) and  $H(\tau)$  is the average rate of heterotrophy.

*Dynamics of energy stores*

Several studies have demonstrated that coral bleaching leads to a reduction in tissue biomass (Porter *et al.* 1989a; Fitt *et al.* 2000;

Loya *et al.* 2001; Grottoli *et al.* 2004; Grottoli *et al.* 2006; Rodrigues & Grottoli 2007; Borell *et al.* 2008). Whether a coral survives or dies from a bleaching event is likely to be determined largely by the dynamics of its energy stores,  $E_s(t)$  (Grottoli *et al.* 2006; Anthony *et al.* 2007; Rodrigues & Grottoli 2007). That is, survival following loss of photosynthetic capacity will depend upon the extent to which energy stores were depleted during the stress event and how rapidly these stores can be rebuilt following the event. In corals and sea anemones, lipid is an important energy-storage compound, and can exceed 20–30% of the tissue biomass (Stimson 1987; Porter *et al.* 1989a; Zamer & Shick 1989; Grottoli *et al.* 2004; Rodrigues & Grottoli 2007). Overall, the dynamics of lipid stores following bleaching depend upon whether a positive or negative energy balance is attained. Where bleaching results in a negative energy budget (i.e. maintenance costs exceed carbon acquisition, eqn 3), lipid stores will be depleted at a rate given by the deficit of the daily energy (carbon) balance, hence

$$\frac{dE_s(t)}{dt} = -kE_B(\text{Chl}, t), \text{ for } E_B(\text{Chl}, t) < 0 \quad \text{eqn 3}$$

where  $k$  is a dimensionless factor of conversion from stored to free energy (see below). The analytical solution is given in the Supporting Information (Appendix S1). Coral tissue biomass and composition (including lipids) vary seasonally in healthy corals (Stimson 1987; Fitt *et al.* 2000; Rodrigues & Grottoli 2007), and therefore restrict the application of the model to the bleaching and subsequent recovery period only. Also, where energy balance is positive, maintenance costs are assumed to be met from newly assimilated carbon at a greater rate than from the catabolism of stored resources (Noonburg *et al.* 1998). Due to space and design constraints within corallites (Leuzinger *et al.* 2003) and potential constraints on tissue thickness (Barnes & Lough 1992), the size of lipid stores will have an upper limit,  $E_{s\max}$ . The build-up of lipid stores is therefore likely to follow a density-dependent function, in which the rate of increase is given by the daily carbon budget,

$$\frac{dE_s(t)}{dt} = mE_B(\text{Chl}, t) \left(1 - \frac{E_s(t)}{E_{s\max}}\right), \text{ for } E_B(\text{Chl}, t) \geq 0 \quad \text{eqn 4}$$

where  $m$  is the efficiency of converting fixed carbon to stored lipids (see Appendix S1, Supporting Information for analytical solution). It is assumed that carbon acquired through photosynthesis and heterotrophic feeding are equally likely carbon sources for lipid synthesis. For simplicity,  $m$  is here assumed to be a constant, but in reality varies with light regime and the intake of food or dissolved nutrients limiting for tissue growth.

#### MORTALITY RISK AS A FUNCTION OF STATUS OF ENERGY STORES

In harsh environments, the probability of survival of organisms is closely linked to their physiological condition (Bloom *et al.* 1985; Gurney *et al.* 1996; Chesson & Huntly 1997; Maltby 1999). Specifically, the point at which resources for the maintenance of basic life functions are exhausted represents a physiologically critical threshold for survival (Gurney *et al.* 1996). For most animals, physiological condition can be characterized by the biochemical composition of body tissues, in particular the content of lipids, proteins and carbohydrates (Kerrigan 1994; Suthers 1998; Grottoli *et al.* 2004; Rodrigues & Grottoli 2007). To express coral mortality risk as an explicit function of the size of energy (lipid) stores, we here use the model developed by Nisbet *et al.* (2000). The model assumes that the

daily hazard rate,  $h(E_s, t)$ , due to physiological condition approaches the baseline hazard,  $h_0$ , at the point where lipid stores are full,  $E_{s\max}$ . Conversely, as  $E_s(t)$  approaches zero  $h(E_s, t)$  increases at a rate that depends on the species' physiological tolerance to resource depletion:

$$h(E_s, t) = h_0 \left[ 1 + \left( \frac{E_{s\max}}{E_s(t) - E_{\text{crit}}} \right)^d \right] \quad \text{eqn 5}$$

where  $d$  is a scaling exponent that determines how steeply hazard rate increases as  $E_s(t)$  approaches the critical size of lipid stores,  $E_{\text{crit}}$ , at which point maintenance costs for survival cannot be met. Hazard rate is here defined as the probability of whole-colony mortality related to changes in energy status – i.e. due to starvation only. The model uses a constant (time-independent) baseline hazard,  $h_0$ , because the 2–3 month time-frame of a thermal stress event is short relative to the baseline life span of coral colonies (years to decades). The analytical solution to the survival function,  $S(t)$ , using  $h(E_s, t)$  as a nested function is intangible, and is here solved numerically (a discrete function) as.

$$S(t+1) = S(t)[1 - h(E_s, t)], \text{ for values of } h(E_s, t) \leq 1. \quad \text{eqn 6}$$

#### FUNCTIONAL RESPONSE CALIBRATION

##### Photosynthetic capacity vs. bleaching status

The relationship between net photosynthetic capacity and bleaching state (eqn 1) was tested based on oxygen respirometry assays of maximum net rate of photosynthesis ( $P_{\text{Net Max}}$ ) and subsequent analyses of concentrations of photopigments (chlorophyll *a*) in populations of natural (*M. monasteriata*) and laboratory-induced (*A. intermedia*) bleaching events. All subcolonies (approximately 40–80 cm<sup>2</sup> tissue surface area) were collected at 3–5 m depth below lowest astronomical tide from 20 to 50 colonies to maximize genotype representation. Corals with different visual bleaching status were assayed for maximum net rates of photosynthesis ( $P_{\text{Net Max}}$ ) at midday irradiances (approximately 800–1200 µmol photons m<sup>-2</sup> s<sup>-1</sup>) and rates of dark respiration ( $R_{\text{Dark}}$ ) at night. Photo-respirometry assays were conducted using standard methods as described by Anthony & Hoegh-Guldberg (2003b). Corals were then snap frozen and stored at -70 °C for later analysis of chlorophyll *a* concentrations per unit surface area, Chl, which were extracted according to standard procedures (Anthony & Hoegh-Guldberg 2003b) and analysed based on equations by (Jeffrey & Humphrey 1975). Equation 1 was fit to the  $P_{\text{Net Max}}$  vs. Chl data using nonlinear, least-squares estimation by the Levenberg–Marquardt method (STATISTICA ver 7.1, StatSoft, USA).

##### Dynamics of lipid stores vs. coral energetics

There is only limited experimental data available to test the relationship between changes in the coral energy budget and the size of colony lipid stores (Porter *et al.* 1989b; Grottoli *et al.* 2004; Anthony *et al.* 2007; Rodrigues & Grottoli 2007). Lipid loss (eqn 3) as a function of bleaching is therefore here based on estimates of conversion coefficients between rates of respiration and lipid catabolism. To convert rates of respiration to lipid loss (coefficient  $k$  in eqn 3), it is here assumed that 1 mg of catabolized lipid corresponds to the respiration of 2.2 mg of carbon (using a specific enthalpy of -39.5 J mg<sup>-1</sup> and a respiratory quotient of 0.72 (Gnaiger & Bitterlich 1984). The coefficient  $k$  is thus estimated to be 0.455 mg lipid mg carbon<sup>-1</sup>. However, the efficiency of converting acquired energy to lipid

anabolism,  $m$ , is under the constraints of an array of factors including limiting nutrients, irradiance and relative dependence on heterotrophy vs. autotrophy (Anthony & Fabricius 2000). Here we assume that carbon acquired through photosynthesis or heterotrophy is equally likely to be converted to lipids, though we acknowledge the possibility that carbon acquired from these sources may be utilized very differently by the coral host. However, rather than constructing a functional response model for lipid anabolism, we here tentatively set  $m$  to a constant  $k/2$  (eqn 5) – i.e. the efficiency of energy conversion via anabolism is half that of catabolism. We note that this value may under- or overestimate the efficiency of lipid anabolism depending on the species, conditions and nutrients availability.

### Mortality risk as a function of lipid stores

To estimate parameters for the hazard model (eqn 5), we used data on mortality rates and tissue lipid contents from an 8-week bleaching experiment for *A. intermedia* (Anthony *et al.* 2007). Here, duplicate experimental populations of 90–110 coral branches from each of two temperature (27 and 31 °C) and two light (100 and 400  $\mu\text{mol m}^{-2} \text{s}^{-1}$ ) treatments were censored daily for mortality and sampled weekly ( $N = 10$  per treatment) for lipid content analyses (Leuzinger *et al.* 2003). Equation 5 was fit to the daily hazard rate vs. lipid content using nonlinear, least-squares estimation similar to analyses for  $P_{\text{Net Max}}$  vs. Chl above.

### MODEL SIMULATIONS

To generate projections of energy balance, lipid-store dynamics and mortality risk over time we coupled all response models (eqns 1–7) using bleaching rate as the primary input variable. To use a generic net photosynthesis vs. chlorophyll-*a* response (eqn 1) for Australian acroporid corals, we averaged the parameter estimates for maximum  $P_{\text{Net Max}}$  and  $a$  across *M. monasteriata* and *A. formosa*. Simulations were then separated into bleaching and post-bleaching (recovery) phases. Five bleaching simulations were run with start populations of 100 corals, each run using different bleaching rates (daily rates of chlorophyll *a* loss varying between 1% and 10%). To also examine how bleaching rate, size of initial lipid stores and heterotrophy influence the proportion of corals that die over time during the bleaching event, we ran simulations with three  $E_{\text{S0}}$  levels (2·0, 1·0 and 0·5 mg lipid  $\text{cm}^{-2}$ , representing full, 50% and 25% initial stores)

and three levels of heterotrophy (0·2, 1·5 and 3·3  $\mu\text{g cm}^{-2} \text{h}^{-1}$ ). In essence, we use the model to explore the sensitivity of mortality risk profiles to different levels of bleaching intensity, initial lipid stores and rates of heterotrophy. Feeding rates were chosen based on values reported for lowest, highest and intermediate feeding rates for acroporid species in varying heterotrophic environments (see above).

For simulations during the recovery phase we also used start populations with 100 corals, and used varying rates of chlorophyll-*a* replenishment. Because the population growth of symbionts is likely to be a density-dependent function, we assumed that chlorophyll *a* growth rates vary over time according to a logistic growth function, that is,  $d\text{Chl}/dt = \gamma \text{ Chl} (1 - \text{Chl}/\text{Chl}_{\text{Max}})$ , where  $\gamma$  is the intrinsic rate of chlorophyll *a* increase at the exponential growth phase of the symbiont population. To simulate periods following a severe bleaching event, we set the chlorophyll *a* concentration at the start of the post-bleaching phase to 5%. Effects of lipid-reserve depletion during 90-day bleaching events on survivorship during the recovery phase were examined for three values of  $E_{\text{S0}}$ : 0·3, 0·4 and 0·5 mg  $\text{cm}^{-2}$  (corresponding to 15%, 20% and 25% of maximum stores), representing the range at which high hazard rates were predicted (Fig. 4). To also test the role of heterotrophy in offsetting mortality following bleaching, the three  $E_{\text{S0}}$  levels were combined with three heterotrophic rates: 0·2, 1·5 and 3·3  $\mu\text{g cm}^{-2} \text{h}^{-1}$ .

## Results and Discussion

### MODEL CALIBRATIONS

#### Photosynthetic capacity as a function of bleaching state

Equation 1 provided a good fit for both species (Fig. 2). The scaling exponent relating  $P_{\text{Net Max}}$  to Chl was significantly lower than unity in both species (Table 2) in accordance with the prediction of a decelerating increase in photosynthetic capacity with increasing chlorophyll *a* concentration. In *M. monasteriata* in particular, up to 40% bleaching did not coincide in a pronounced decline in  $P_{\text{Net Max}}$ . Maximum rate of photosynthesis at zero chlorophyll *a* content,  $P_{0 \text{ Max}}$ , was not significantly different from zero in initial regression analyses, and was omitted from further analyses. Interestingly, rate of

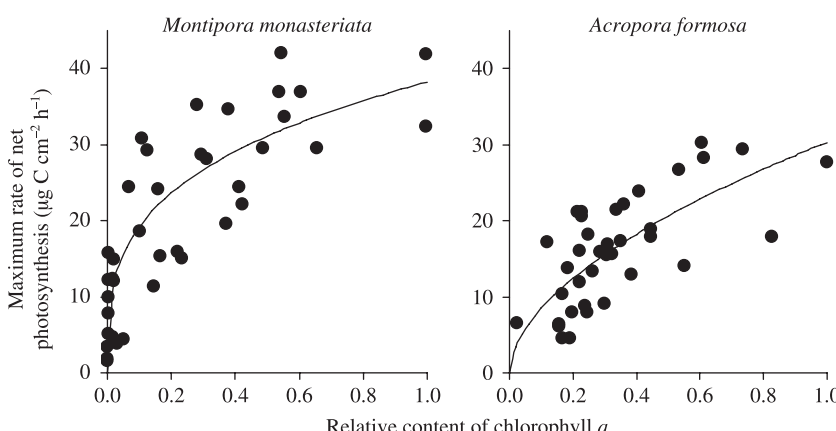


**Fig. 2.** Relationship between photosynthetic capacity and bleaching status (as chlorophyll *a* content) in two acroporid coral species. The function  $P_{\text{max}} = P_{\text{Ch/Max}} \text{Chl}^a$  (eqn 1) provided a good fit to both datasets, explaining 73% of the variation in chlorophyll *a* for *M. monasteriata* and 53% for *A. formosa* ( $P$ -values  $< 0\cdot001$  for both regressions). Parameter estimates are given in Table 2.

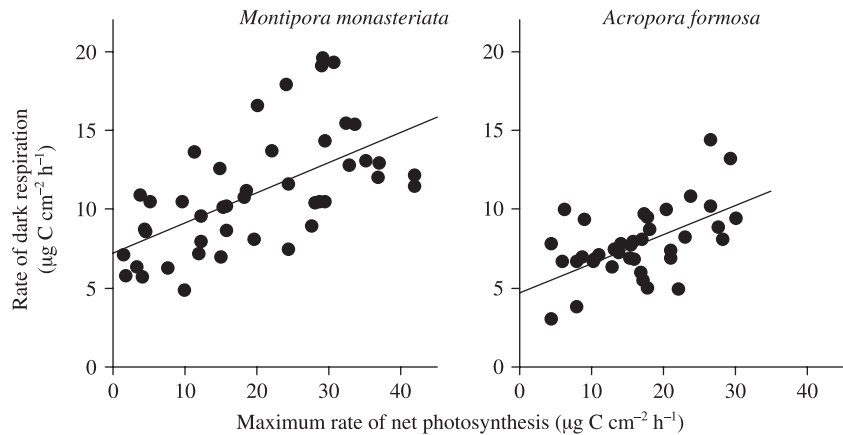


**Fig. 3.** Relationship between rate of dark respiration ( $R_{\text{Dark}}$ ) and photosynthetic capacity ( $P_{\text{Net Max}}$ ). A linear model provided a good fit to the data for both *M. monasteriata* ( $R^2 = 0.36$ ,  $P < 0.05$ ) and *A. formosa* ( $R^2 = 0.38$ ,  $P < 0.05$ ). See Table 2 for summary of parameter estimates from linear regression analyses.

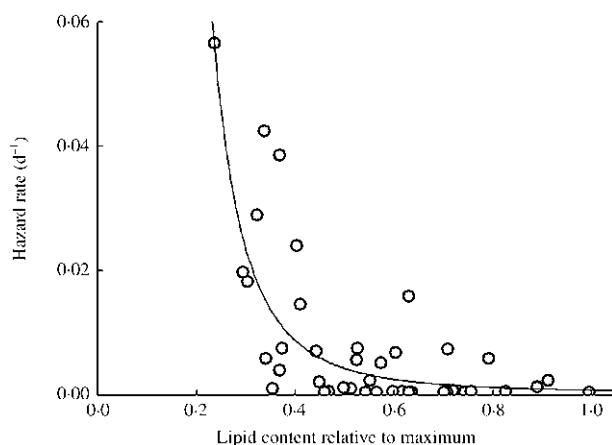


**Fig. 4.** Relationship between tissue lipid content and daily hazard rate (mortality risk) in *Acropora intermedia*. Critical energy stores ( $E_{\text{crit}}$ ) were set to 5% (see text). The solid line is eqn 4 fitted to data from Anthony *et al.* (2007) on observed hazard rates vs. lipid content. Equation 6 explained 63% of the variation in lipid contents. Dashed lines indicate 95% confidence bands.

dark respiration ( $r_{\text{Dark}}$ ) showed no relationship with chlorophyll *a* content but increased approximately linearly with  $P_{\text{Net Max}}$ , from approximately  $5-7 \mu\text{g C cm}^{-2} \text{h}^{-1}$  at zero rate of net photosynthesis to  $12-15 \mu\text{g C cm}^{-2} \text{h}^{-1}$  at maximum photosynthetic capacity (Fig. 3). Therefore, the respiration term in eqn 2 was substituted by the function.

$$R_{\text{Dark}}(\text{Chl}, t) = bP_{\text{Net Max}}(\text{Chl}, t) + R_{\text{Base}} \quad \text{eqn 7}$$

where  $b$  is the regression coefficient and  $R_{\text{Base}}$  is the minimum rate of respiration. A summary of all parameter estimates from regression analyses are given in Table 2.

#### Mortality vs. lipid stores

The hazard model (eqn 5) provided a good fit to the lipid and mortality data for *A. intermedia* (Anthony *et al.* 2007), explaining around 63% of the variation in coral energy stores (Fig. 4). The best model fit was obtained when  $E_{\text{crit}}$  was set to

< 5% of  $E_{\text{S max}}$ . The parameter estimates were both significantly different from zero and determined with high precision ( $h_0 = 0.00036 \pm \text{SE } 0.0002 \text{ day}^{-1}$ ,  $d = 3.5 \pm \text{SE } 0.38$ , Table 2). This functional relationship indicated that hazard rates of *A. intermedia* are largely unaffected by reductions in lipid stores down to approximately 40% of maximum, but then increase dramatically with further reductions in lipids.

#### CORAL MORTALITY RISK

##### Effects of bleaching rate on lipid stores

Initial model simulations for the bleaching phase using corals with a low constant heterotrophic rates ( $H(t) = 0.2 \mu\text{g cm}^{-2} \text{h}^{-1}$ ) and maximum initial energy stores ( $E_{\text{S0}} = 2 \text{ mg cm}^{-2}$ ), indicated that the timing of the onset of lipid losses (Fig. 5c) and associated mortalities (Fig. 5d) was strongly influenced by bleaching rate (Fig. 5a) via its effects on coral energy balance (Fig. 5b). At the highest bleaching rates (10%, i.e. complete chlorophyll *a* loss in 10 days), the gradual depletion of energy stores did not start until about 8 days into the event (Fig. 5c) – i.e. at the point where the daily energy balance shifted from positive to negative (Fig. 5b). For corals with full lipid stores showing the highest bleaching rate, complete depletion would occur over approximately 2 months (Fig. 5c). Consequently, at the highest bleaching rates, the onset of high mortalities did not occur until 40–50 days after the onset of bleaching. At slower bleaching rates, associated rates of lipid-store depletion were reduced accordingly as energy balance remained positive for longer (Fig. 5b). For bleaching rates of 2.5–10% chlorophyll *a* loss per day, the transition between low- and high-mortality risk zones was very abrupt; with increases in accumulated mortality from approximately 0% to 100% occurring over a time window of only 5–10 days in all cases (Fig. 5d). At the slowest bleaching rates of 1.5% and 1.0% chlorophyll-*a* loss per day, a positive energy budget was maintained for a minimum of 60 days and mortality rates were < 10% at the end of the 90-day run. Thus, the model shows that if bleaching events are slow enough, corals with initial lipid stores would have very high survivorship following warming events that were 60 days in duration or shorter.

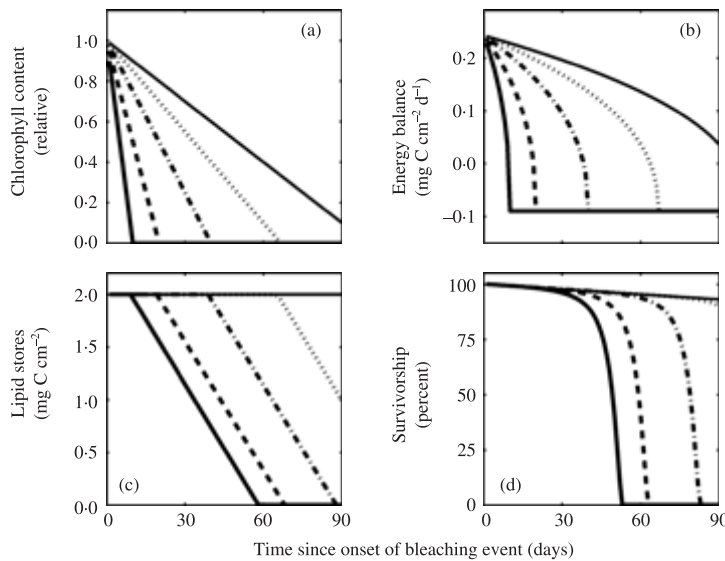


**Fig. 5.** Changes in (a) chlorophyll *a* during a 90-day simulated bleaching event and predicted modelled effects on (b) daily energy balance, (c) lipid stores and (d) survivorship in acroporid corals with low and constant heterotrophic capacity,  $H(t) = 0.2 \mu\text{g cm}^{-2}\text{h}^{-1}$ , and maximum initial lipid stores before bleaching,  $E_{S0} = 2 \text{ mg cm}^{-2}$ . Legend indicates bleaching rates as daily percentage loss of chlorophyll *a* relative to maximum.

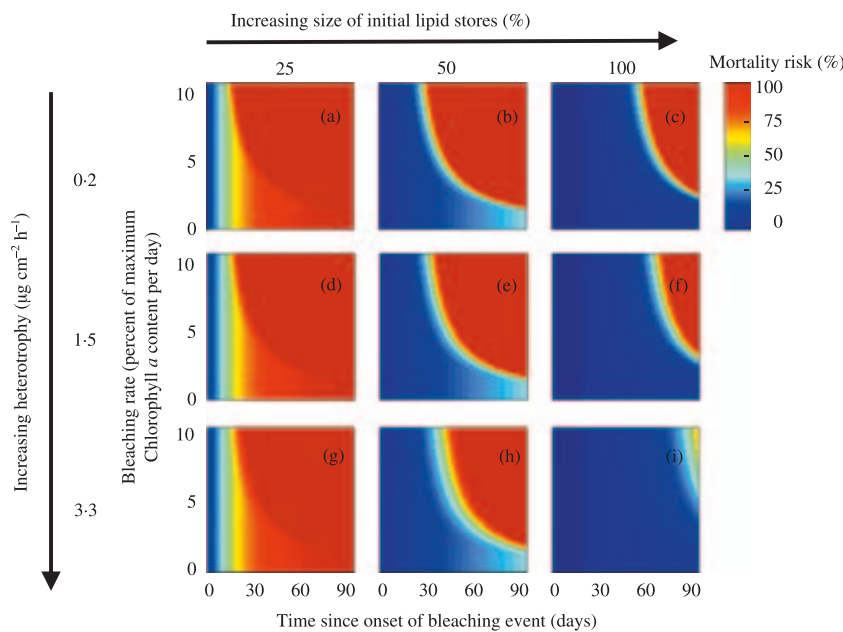


**Fig. 6.** Effects of the size of initial lipid stores (before bleaching,  $E_{S0}$ ), rate of heterotrophy and bleaching rate ( $d\text{Chl}_n(t)/dt$ ) on accumulated coral mortality risk (colour bar, %) during a 3-month bleaching event. Initial percentages of lipid content of 25%, 50% and 100% correspond to 0.5, 1.0 and 2.0 mg lipid  $\text{cm}^{-2}$ , respectively.

#### Effects of initial energy stores and heterotrophic rate

Varying the initial lipid stores ( $E_{S0}$ , simulating different energy-costly disturbances before the event or natural variations in lipids that occur with the seasonal cycle) had dramatic consequences for coral survivorship profiles (Fig. 6). Reducing  $E_{S0}$  to 50% and 25% of maximum energy reserves (1.0 and 0.5 mg  $\text{cm}^{-2}$ , respectively) meant that the onset of critically high mortalities occurred 20 and 40 days earlier than for corals with full initial energy reserves (2 mg  $\text{cm}^{-2}$ ), respectively. Moreover, results showed that for corals with the smallest lipid stores (25% of maximum) at the start of the bleaching event, rates of chlorophyll *a* loss as low as 1–2% per day can

incur 50–60% mortality within 20 days (Fig. 6a,d,g). Assuming that feeding rates do not change in response to bleaching, the underlying mechanism is that once energy stores are lowered to the extent that hazard rate starts increasing steeply (Fig. 4) even the highest heterotrophic rates are insufficient to replenish energy stores in time to counteract the onset of mass mortality.

For corals with full energy reserves, moderate to high rate of heterotrophic carbon (1.5–3.3  $\mu\text{g cm}^{-2}\text{h}^{-1}$ ) could delay the onset of critically high mortalities by 2–4 weeks relative to that of corals almost fully dependent on phototrophy (0.2  $\mu\text{g cm}^{-2}\text{h}^{-1}$ , compare Fig. 5c,f,i). The role of heterotrophy in counteracting energy loss during bleaching events is thus highly dependent

on energy reserves before the onset of the event, and on bleaching severity. However, this interpretation assumes that feeding rates do not increase during bleaching to compensate for reductions in photosynthetically acquired fixed carbon. Recent work by Grottoli *et al.* (2006) shows that for *M. capitata* corals, feeding rates increase dramatically in bleached corals, fully compensating for any reductions in photosynthetically acquired fixed carbon and maintaining energy reserves. In addition, both *M. monasteriata* (Dove *et al.* 2006) and *M. capitata* (Rodrigues & Grottoli 2007) have the unique characteristic of losing chlorophyll *a* but not zooxanthellae cells when bleached. If this unique trait is symptomatic of other similarities in coral physiology among species of *Montipora*, then it is possible that the high heterotrophic capacity observed in *M. capitata* may be present in other *Montipora* species. Although our model assumes a constant heterotrophic rate during bleaching, the broad envelope of feeding capacities used in separate simulations indicates that heterotrophy plays a key role in offsetting mortality risk associated with bleaching. Even for corals with maximum initial lipid stores, mortality risk continues to decrease with increases in heterotrophy.

#### CORAL SURVIVORSHIP FOLLOWING BLEACHING EVENTS

The relationship between replenishment of photopigments, lipid stores and survivorship for bleached corals with a low heterotrophic rate ( $0.2 \mu\text{g C cm}^{-2} \text{h}^{-1}$ ) and partly depleted lipid stores (here using 80% depletion,  $0.4 \text{ mg lipid cm}^{-2}$ , as an example) is shown in Fig. 7. As expected, in corals that rely predominantly on phototrophy, survivorship is directly related to rate of chlorophyll-*a* recovery and the associated rate of lipid-store replenishment. With a zero rate of chlorophyll-*a* recovery, none of the corals surviving the

bleaching phase recovered their lipid stores, and died within 40 days after the bleaching phase (Fig. 7a,d). Conversely, corals able to restore their photo-pigments within one month following the bleaching event (Fig. 7a) showed 50% survivorship (Fig. 7d).

Analyses demonstrated that survivorship during periods following bleaching was particularly sensitive to variation in the size of lipid stores at the end of the bleaching event (Fig. 8). For high chlorophyll-*a* recovery rates, a shift in lipid stores from 15% to 25% of maximum led to increases in survival from 20% to 60% for corals with low heterotrophic rates (Fig. 8a–c) and to increases in survival from 40% to 70% in corals with high heterotrophic rates (Fig. 8g–i). Overall, higher lipid reserves at the onset of recovery meant that 20–40% of corals with low rates of chlorophyll-*a* replenishment ( $\gamma = 0.3\%$  and  $1.0\%$ ) would now survive after bleaching. With rates of heterotrophy increasing from  $0.2$  to  $3.3 \mu\text{g cm}^{-2} \text{h}^{-1}$ , survivorship of these groups would increase to 50–55% (Fig. 7c,i). Overall, our results indicate that rate of heterotrophy, the size of remaining lipid reserves and rate of chlorophyll-*a* recovery act synergistically in promoting post-bleaching survivorship. The underlying mechanism is that for corals that are unable to increase their feeding rates, depletion of their lipid stores to critically low levels leads to run-away mortality. It is important to note that the effect of heterotrophy on chlorophyll-*a* recovery rate is not accounted for here. In reality, nutrient supply via feeding is likely to enhance the mitotic index of symbionts (Hoegh-Guldberg 1994) leading to accelerated chlorophyll recovery. This may also play a role in tissue and lipid recovery.

#### Conclusions

The energetics approach used here, linking coral bleaching to mortality risk, provides a strong framework for understanding

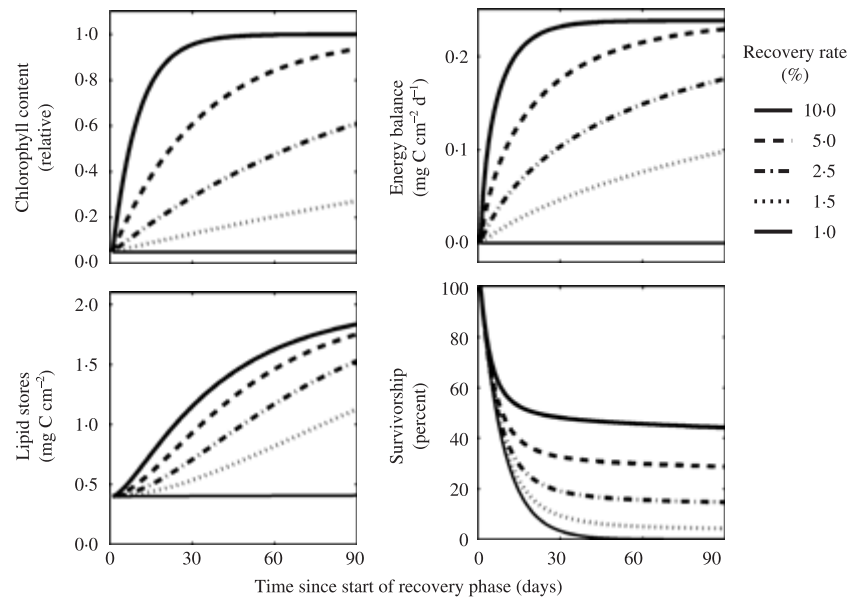


**Fig. 7.** Relationship between rate of chlorophyll *a* recovery, restoration of lipid stores and survivorship for predominantly phototrophic corals,  $H(t) = 0.2 \mu\text{g C cm}^{-2} \text{h}^{-1}$ , with partly depleted lipid stores at the end of the bleaching event (here set to  $E_{s0} = 0.4 \text{ mg cm}^{-2}$  as an example). Rate of chlorophyll *a* recovery was assumed to follow a density-dependent (logistic) growth function. The intrinsic rate of chlorophyll *a* increase ( $\gamma$ , the ‘recovery rate’), was here varied from 0% to 10% (figure legend).

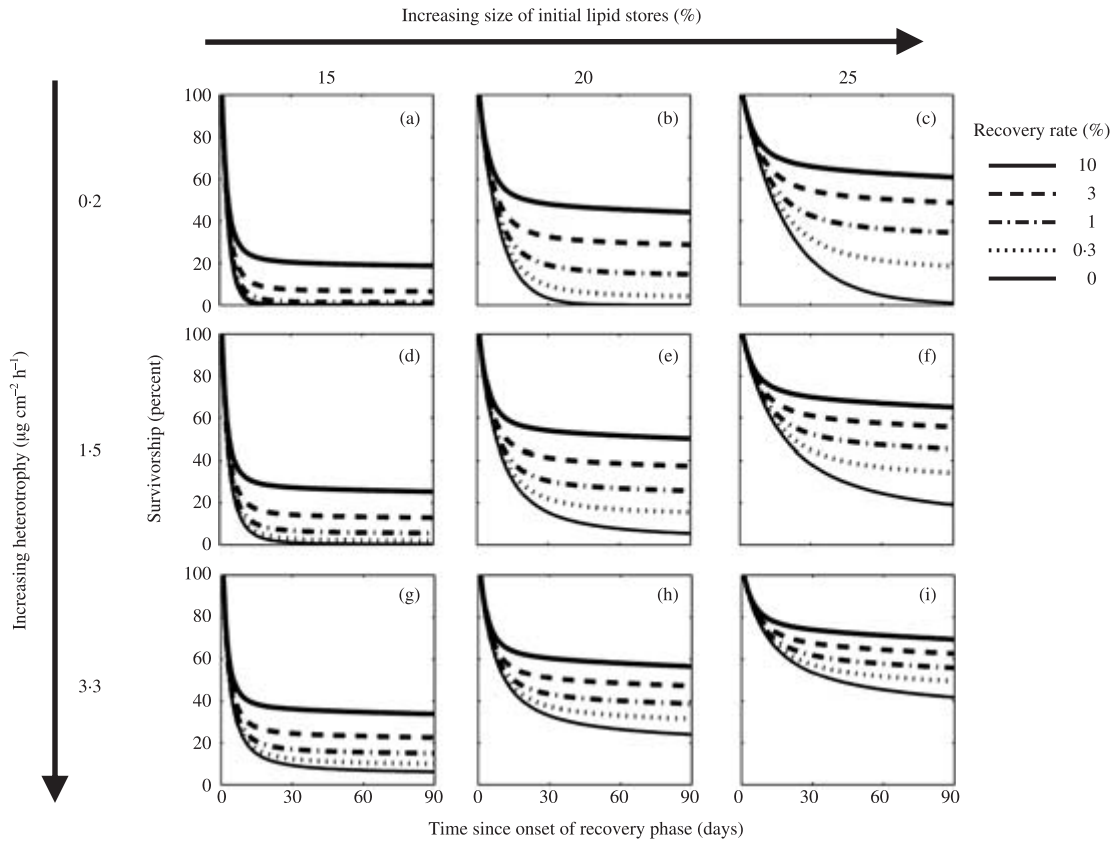


**Fig. 8.** Effects of varying lipid-store depletion and rate of heterotrophy on survivorship of corals during a 3-month recovery phase following a bleaching event. Here, the size of lipid stores on the first day of the recovery phase ( $E_s$  for the last of the bleaching phase) was varied between three levels: 0.3, 0.4 and 0.5 mg lipid  $\text{cm}^{-2}$ , representing 15%, 20% and 25% of the maximum lipid content, at which points of high hazard rates are expected (Fig. 4). The intrinsic rate of chlorophyll *a* increase ( $\gamma$ ), the 'recovery rate', was here varied from 0% to 10% (figure legend). Heterotrophy was varied as in Fig. 6.

how bleaching severity (i.e. bleaching rate and/or event duration), coral condition and resource environment determine mortality levels during and following bleaching events. Our model analyses demonstrated a number of key points. First, the time between the onset of severe bleaching (i.e. a high rate of chlorophyll-*a* loss) and the onset of a high mortality rate is influenced by two main factors: (i) size of lipid stores before the bleaching event and (ii) capacity to acquire energy (carbon) through heterotrophy. Assuming that bleaching rate is linear, there is an inverse relationship between initial lipid stores and the timing of the onset of high mortality rates. Under high rates of bleaching, corals with full initial lipid stores will survive for twice as long as corals with half-depleted lipid stores. This has two implications. (i) Other stressors that cause a reduction in tissue lipid content before a bleaching event will strongly influence how severely a coral community will be affected by bleaching. Examples of events that could result in lowered lipid stores before the onset of bleaching events in summer include extreme tidal events (Anthony & Kerswell 2007), winter bleaching (Hoegh-Guldberg *et al.* 2005), anomalous spring temperatures (Weeks *et al.* 2008), flooding events (Devlin & Brodie, 2005) and spawning (Leuzinger *et al.* 2003). (ii) The timing of the bleaching event, likely to become increasingly variable under climate-change

scenarios, relative to the natural seasonal cycle in lipid reserves could influence how severely a coral community is affected by bleaching.

Interestingly, a high heterotrophic capacity could significantly offset the effects of bleaching on the coral energy balance during both the bleaching and the recovery phases, particularly for corals with moderate to large lipid stores. Consequently, the time between the onset of bleaching and the onset of high rates of mortality can be delayed significantly if initial energy reserves are moderate to high and/or for highly heterotrophic species in locations with high resource availability. Similarly, during the recovery phase for severely bleached corals, a high rate of heterotrophy can shift the energy balance from negative to positive and help restore lipids at a rate sufficient to reduce mortality rates. Clearly, the role of heterotrophy in reducing mortality rates during bleaching and recovery phases has implications for patterns of bleaching-induced stress and mortality between reefs with varying trophic resources. In particular, it may have implications for variations in bleaching-induced mortality between coastal and offshore reefs. The enhancement of recovery rates as a result of heterotrophy may be even greater than demonstrated in our models for species with the capacity to increase their feeding rates during bleaching and recovery.

Our model uses bleaching rate as the input variable, and does not explicitly relate the rate of bleaching to the array of factors that cause bleaching – primarily thermal stress (Berkelmans 2002) and high irradiance (Dunne & Brown, 2001). Extending the model to include a formal account of how environmental variation relates to bleaching rate would allow assessments of mortality risk from environmental data in real time. Existing frameworks that relate temperature anomalies to bleaching risk (e.g. NOAA's Coral Reef Watch (Strong *et al.* 2004) and *ReefTemp* (Maynard *et al.* 2008) could be coupled with the model presented here to enable large-scale mortality risk predictions. Predicting coral mortality risk during bleaching events would fine-tune research and monitoring efforts. As a result, more informed decisions can be made with regard to the allocation of management resources to the mitigation of anthropogenic stressors that can work to increase recovery timeframes following disturbances.

## Acknowledgements

This study was funded by the Australian Research Council (ARC) via the ARC Centre of Excellence for Coral Reef Studies, a Marine and Tropical Sciences Research Facility grant from the Australian Government. Authors thank S. Dove, O. Hoegh-Guldberg and R. Berkelmans for critical reading and valuable comments.

## References

Anthony, K.R.N. (1999) Coral suspension feeding on fine particulate matter. *Journal of Experimental Marine Biology and Ecology*, **232**, 85–106.

Anthony, K.R.N. (2000) Enhanced particle-feeding capacity of corals on turbid reefs (Great Barrier Reef, Australia). *Coral Reefs*, **19**, 59–67.

Anthony, K.R.N. & Connolly, S.R. (2004) Environmental limits to growth: physiological niche boundaries of corals along turbidity-light gradients. *Oecologia*, **141**, 373–384.

Anthony, K.R.N. & Kerswell, A. (2007) Coral mortality following extreme low tides and high solar radiation. *Marine Biology*, **151**, 1623–1631.

Anthony, K.R.N. & Fabricius, K.E. (2000) Shifting roles of heterotrophy and autotrophy in coral energetics under varying turbidity. *Journal of Experimental Marine Biology and Ecology*, **252**, 221–253.

Anthony, K.R.N. & Hoegh-Guldberg, O. (2003a) Kinetics of photoacclimation in corals. *Oecologia*, **134**, 23–31.

Anthony, K.R.N. & Hoegh-Guldberg, O. (2003b) Variation in coral photosynthesis, respiration and growth characteristics in contrasting light microhabitats: an analogue to plants in forest gaps and understoreys? *Functional Ecology*, **17**, 246–259.

Anthony, K.R.N., Connolly Sean, R. & Hoegh-Guldberg, O. (2007) Bleaching, energetics and coral mortality risk: effects of temperature, light, and sediment regime. *Limnology and Oceanography*, **52**, 716–726.

Baker, A.C. (2001) Reef corals bleach to survive change. *Nature*, **411**, 765–766.

Barnes, D.J. & Chalker, B.E. (1990) Calcification and photosynthesis in reef-building corals and algae. *Ecosystems of the World: Coral Reefs* (ed. Z. Dubinsky), pp. 109–131. Elsevier, Amsterdam.

Barnes, D.J. & Lough, J.M. (1992) Systematic variations in the depth of skeleton occupied by coral tissue in massive colonies of *Porites* from the Great Barrier Reef. *Journal of Experimental Marine Biology and Ecology*, **159**, 113–128.

Berkelmans, R. (2002) Time-integrated thermal bleaching thresholds of reefs and their variation on the Great Barrier Reef. *Marine Ecology Progress Series*, **229**, 73–82.

Berkelmans, R. & van Oppen, M.J.H. (2006) The role of zooxanthellae in the thermal tolerance of corals: a 'nugget of hope' for coral reefs in an era of climate change. *Proceedings of the Royal Society B-Biological Sciences*, **273**, 2305–2312.

Berkelmans, R. & Willis, B.L. (1999) Seasonal and local spatial patterns in the upper thermal limits of corals on the inshore Central Great Barrier Reef. *Coral Reefs*, **18**, 219–228.

Berkelmans, R., De'ath, G., Kininmonth, S. & Skirving, W.J. (2004) A comparison of the 1998 and 2002 coral bleaching events on the Great Barrier Reef: spatial correlation, patterns, and predictions. *Coral Reefs*, **23**, 74–83.

Bloom, A.J., Chapin III, F.S. & Mooney, H.A. (1985) Resource limitation in plants – an economic analogy. *Annual Review of Ecological Systems*, **16**, 363–392.

Borell, E.M., Yuliantri, A.R., Bischof, K. & Richter, C. (2008) The effect of heterotrophy on photosynthesis and tissue composition of two scleractinian corals under elevated temperature. *Journal of Experimental Marine Biology and Ecology*, **364**, 116–123.

Brown, B.E., Dunne, R.P., Scoffin, T.P. & Le Tissier, M.D.A. (1994) Solar damage in intertidal corals. *Marine Ecology Progress Series*, **105**, 219–230.

Chalker, B.E., Dunlap, W.E. & Oliver, J.K. (1983) Bathymetric adaptations of reef-building corals at Davies Reef, Great Barrier Reef, Australia. II. Light saturation curves for photosynthesis and respiration. *Journal of Experimental Marine Biology and Ecology*, **73**, 37–56.

Chesson, P. & Huston, N. (1997) The roles of harsh and fluctuating conditions in the dynamics of ecological communities. *American Naturalist*, **150**, 519–553.

Crossland, C.J., Barnes, D.J. & Borowitzka, M.A. (1980) Diurnal lipid and mucus production in the staghorn coral *Acropora acuminata*. *Marine Biology*, **60**, 81–90.

Devlin, M.J. & Brodie, J. (2005) Terrestrial discharge into the Great Barrier Reef Lagoon: nutrient behavior in coastal waters. *Marine Pollution Bulletin*, **51**, 9–22.

Donner, S.D., Knutson, T.R. & Oppenheimer, M. (2007) Model-based assessment of the role of human-induced climate change in the 2005 Caribbean coral bleaching event. *Proceedings of National Academy of Sciences*, **104**, 5483–5488.

Dove, S., Ortiz, J.C., Enriquez, S., Fine, M., Fisher, P., Iglesias-Prieto, R., Thornhill, D. & Hoegh-Guldberg, O. (2006) Response of holosymbiont pigments from the scleractinian coral *Montipora monasteriata* to short-term heat stress. *Limnology and Oceanography*, **51**, 1149–1158.

Dunne, R.P. & Brown, B.E. (2001) The influence of solar radiation on bleaching of shallow water reef corals in the Andaman Sea, 1993–1998. *Coral Reefs*, **20**, 201–210.

Dunne, R.P., Gleason, M.W. & Wellington, G.M. (1994) Radiation and coral bleaching. *Nature*, **368**, 697.

Enriquez, S., Mendez, E.R. & Iglesias-Prieto, R. (2005) Multiple scattering on coral skeletons enhances light absorption by symbiotic algae. *Limnology and Oceanography*, **50**, 1025–1032.

Falkowski, P.G., Jokiel, P.L. & Kinzie III, R.A. (1990) Irradiance and corals. *Ecosystems of the World: Coral Reefs* (ed. Z. Dubinsky), pp. 89–107. Elsevier, Amsterdam.

Frerrier-Pages, C., Allemand, D., Gattuso, J.P., Jaubert, J. & Rassoulzadegan, R. (1998) Microheterotrophy in the zooxanthellate coral *Stylophora pistillata*: Effects of light and ciliate density. *Limnology and Oceanography*, **43**, 1639–1648.

Fitt, W.K., McFarland, F.K., Warner, M.E. & Chilcoat, G.C. (2000) Seasonal patterns of tissue biomass and densities of symbiotic dinoflagellates in reef corals and relation to coral bleaching. *Limnology and Oceanography*, **45**, 677–685.

Gleason, M.W. & Strong, A.E. (1995) Applying McSST to Coral-Reef Bleaching. *Adv. Space Res.*, **16**, 151–154.

Gnaiger, E. & Bitterlich, G. (1984) Proximate biochemical composition and calorific content calculated from elemental CHN analysis: a stoichiometric concept. *Oecologia*, **62**, 289–298.

Grottoli, A.G., Rodrigues, L.J. & Juarez, C. (2004) Lipids and stable carbon isotopes in two species of Hawaiian corals, *Porites compressa* and *Montipora verrucosa*, following a bleaching event. *Marine Biology*, **145**, 621–631.

Grottoli, A.G., Rodrigues, L.J. & Palardy, J.E. (2006) Heterotrophic plasticity and resilience in bleached corals. *Nature*, **440**, 1186–1189.

Gurney, W.S.C., Middleton, D.A.J., Nisbet, R.M., McCauley, E., Murdoch, W.M. & DeRoos, A. (1996) Individual energetics and the equilibrium demography of structured populations. *Theoretical Population Biology*, **49**, 344–368.

Hoegh-Guldberg, O. (1994) Population dynamics of symbiotic zooxanthellae in the coral *Pocillopora damicornis* exposed to elevated ammonium ((NH<sub>4</sub>)<sub>2</sub>SO<sub>4</sub>) concentrations. *Pacific Science*, **48**, 263–272.

Hoegh-Guldberg, O. (1999) Climate change, coral bleaching and the future of the world's coral reefs. *Marine and Freshwater Research*, **50**, 839–866.

Hoegh-Guldberg, O. & Jones, R.J. (1999) Photoinhibition and photoprotection in symbiotic dinoflagellates from reef-building corals. *Marine Ecology Progress Series*, **183**, 73–86.

Hoegh-Guldberg, O., Fine, M., Skirving, W., Johnstone, R., Dove, S. & Strong, A. (2005) Coral bleaching following wintry weather. *Limnology and Oceanography*, **50**, 265–271.

Received 21 April 2008; accepted 3 December 2008

Received 21 April 2008; accepted 10 June 2008  
Handling Editor: Frank Messing

## Supporting Information

Additional Supporting Information may be found in the online version of this article:

## Appendix S1 Lipid Store Dynamics

Please note: Wiley-Blackwell are not responsible for the content or functionality of any supporting materials supplied by the authors. Any queries (other than missing material) should be directed to the corresponding author for the article.